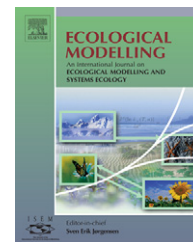


available at www.sciencedirect.comjournal homepage: www.elsevier.com/locate/ecolmodel

Soil drying in a tropical forest: Three distinct environments controlled by gap size

T.R. Marthews^{a,*}, D.F.R.P. Burslem^a, S.R. Paton^b, F. Yangüez^b, C.E. Mullins^a

^a School of Biological Sciences, University of Aberdeen, Aberdeen AB24 3UU, UK

^b Smithsonian Tropical Research Institute (S.T.R.I.), Apartado 0843-03092, Ancón, Panama City, Panama

ARTICLE INFO

Article history:

Received 27 July 2007

Received in revised form

12 May 2008

Accepted 19 May 2008

Published on line 26 June 2008

Keywords:

Boundary layer modelling

Filter-paper technique

Forest regeneration

Gap dynamics

Litter

Panama

Root water extraction

SWEAT

ABSTRACT

Soil water and temperature regimes in the tropical moist forest on Barro Colorado Island, Panama, were simulated directly from meteorological data using the model SWEAT. Separate field observations from root-exclusion, litter-removal and control treatments in one small and one large forest gap were used for calibration and validation. After irrigating all treatments to field capacity, soil matric potential and temperature were measured over 17 days at four depths ≤ 50 mm using the filter-paper technique and bead thermistors. Understorey environments were also simulated under the same initial conditions. The results suggest that three distinct scenarios, controlled by gap size, describe how the above- and below-ground processes controlling soil drying are coupled: (1) in the large gap, root water extraction by surrounding trees is negligible so soil drying is dominated by evaporation from the soil surface. Soil temperature is dominated by direct solar heating and cooling due to evaporation. (2) In the small gap, root water extraction dominates soil drying with soil evaporation playing a minor role. Soil temperature is still dominated by direct sunlight with some cooling due to evaporation. (3) In the understorey, root water extraction dominates soil drying. Soil temperature is dominated by heat conduction from deep soil layers with some evaporation and sensible heat transfer. The contrasting soil drying regimes imposed by variation in canopy structure enhance micro-environmental heterogeneity and the scope for differential germination and seedling establishment in coexisting tropical tree species.

© 2008 Elsevier B.V. All rights reserved.

1. Introduction

Canopy gaps are a driving force behind the regeneration of tropical forests (Whitmore, 1998). Taking large gaps and the understorey as two ends of a gradient of environmental conditions, tree species seem to be adapted only to certain parts of the gradient. This gradient is associated with a spectrum of species-specific shade tolerance at the seedling stage (Swaine and Whitmore, 1988 as updated by Kyre et al., 1999, reviewed in Poorter, 2005).

However, taking a seed's eye view (Pearson et al., 2003b), the main environmental requirements for seed germination are suitable temperature and water availability (Gumerson, 1986; Bradford, 2002). These are both strongly affected by the timing and duration of dry and wet periods in seasonal forests (Garwood, 1983; Engelbrecht et al., 2001, 2006; Dalling and Hubbell, 2002; Poorter, 2005), which affect gap and understorey areas differently. Engelbrecht et al. (2001, 2006) showed that survival of newly emerging pioneer species was reduced significantly by dry spells of as little as 6 days in 225 m² litter-free

* Corresponding author. Tel.: +44 1224 272000.

E-mail address: Toby.Marthews@lsce.ipsl.fr (T.R. Marthews).

0304-3800/\$ – see front matter © 2008 Elsevier B.V. All rights reserved.

doi:10.1016/j.ecolmodel.2008.05.011

gaps in a tropical moist forest in Panama. This study highlighted the potential importance of short dry spells in the wet season as an environmental filter regulating tree seedling recruitment (Dalling and Hubbell, 2002; Poorter, 2005).

Soil water regimes and the effects of canopy structure and leaf litter in tropical forests are inadequately known, as has been pointed out by many authors (e.g. Grubb, 1996; Dalling and Hubbell, 2002; Poorter, 2005). Dry or wet conditions above the canopy of a forest do not necessarily result in dry or wet conditions in the soil below because of canopy interception (Bruijnzeel, 1989; Leigh, 1999) and the effects of topography (Daws et al., 2002, 2005b), soil properties (Marshall et al., 1996), roots (Ostertag, 1998) and litter (Molofsky and Augspurger, 1992; Grubb, 1996; Dalling and Hubbell, 2002). Even on flat ground in forest gaps, roots and litter are usually present and modify the soil environment and how quickly it dries (Marshall et al., 1996; Sayer, 2005), resulting in a complex spatial pattern of soil water availability. Furthermore, there is conflicting evidence on whether soil in gaps is drier or wetter than understorey soil in tropical forests (Poorter and Hayashida-Oliver, 2000; Poorter, 2005) and the effects of root water extraction are little known.

To describe the effects of wet and dry spells in natural gaps or understorey areas, the processes governing soil drying must be characterised far more precisely than hitherto. In this study on Barro Colorado Island, Panama (BCI), soil drying after simulated rainfall (irrigation) during the dry season was measured in a large and a small natural gap at 0–5, 5–10, 15–20 and

45–55 mm depths. A known weakness of many soil transport models is that they simulate water movement separately from heat flow, and therefore unreliably simulate the top 50 mm of the soil column where water vapour transfer is more significant (crucial for predictions of seedling emergence). Therefore, the model SWEAT, which takes a coupled approach to the flow of heat, water and water vapour, was used to predict values of soil dryness (matric potential) and temperature. This allowed the following questions to be addressed: (1) How do soil water availability and temperature change as soil dries? (2) What are the effects of litter and roots? (3) How do soil water and temperature regimes differ between the understorey, a small gap and a large gap? (4) How does soil drying affect germination and seedling mortality?

2. Methods

2.1. Study area

Barro Colorado Island (BCI, 9°09'N 79°51'W) is a 15.6 km² island in the Canal Zone of Panama (Fig. 1) administered by the Smithsonian Tropical Research Institute. BCI supports a Tropical Moist Forest (Holdridge Life-Zone System, Holdridge et al., 1971) with a canopy 24.6 ± 9.5 m high (mean ± 1S.D., S. Hubbell, L. Comita and R. Condit, unpublished data), approximately half of which has been undisturbed since at least ca. 1600 (Foster and Brokaw, 1982; Fig. 1). Annual rainfall

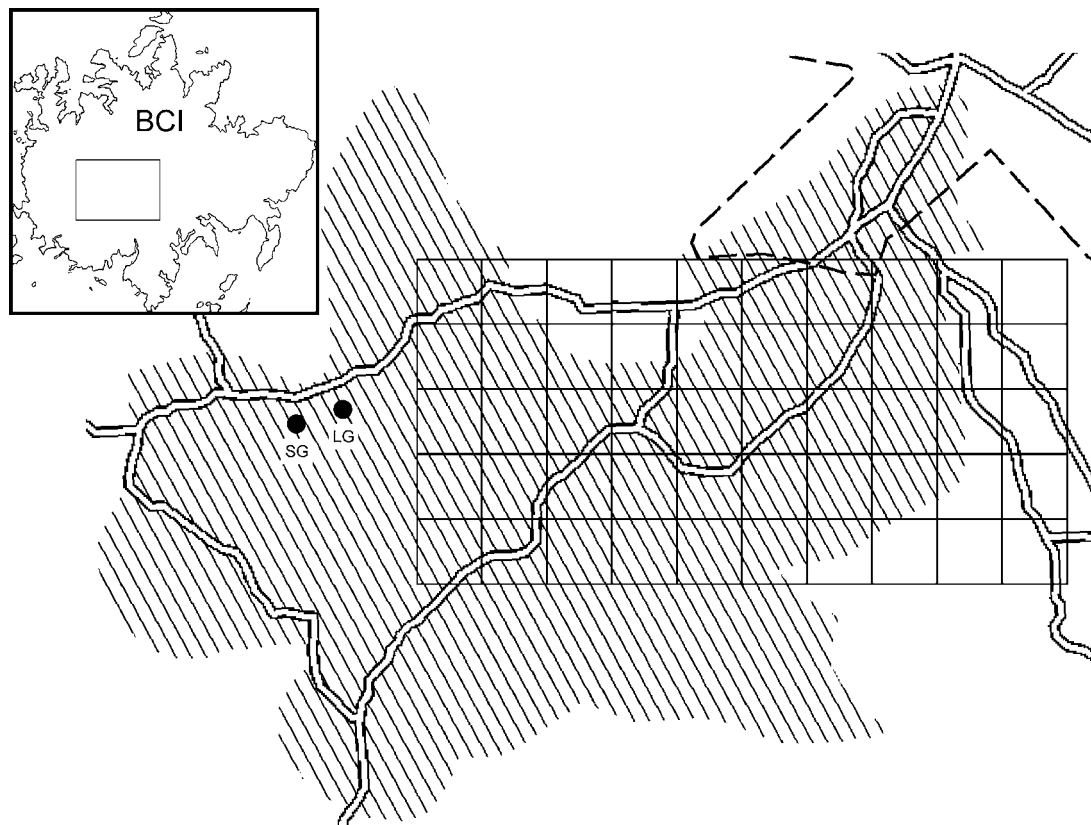


Fig. 1 – Barro Colorado Island (BCI) in Panama and the small gap (SG, Zetek 9.4) and large gap (LG, Zetek 8.6) study sites. Trails are marked, the Ava soil type (Baillie et al., 2007) is shaded and the neighbouring 0.5 km × 1.0 km Forest Dynamics Plot (Hubbell and Foster, 1983; Condit, 1998) is shown as a grid (oriented with long side East-West). The broken line shows approximately the division between old (to SW) and young forest (Foster and Brokaw, 1982).

is 2644 ± 443 mm (mean \pm 1S.D., 1925–2005 data, T-ESP, 2006). There are two seasons, a dry season (21 December–4 May, mean dates 1954–2005, T-ESP, 2006), when rainfall averages 2.1 mm/day, and a wet season, with rainfall 10.1 mm/day (1925–2005 data, T-ESP, 2006). Temperatures range from 23.1 to 27.2 °C in November to 23.4 to 29.7 °C in March in a clearing at 1 m above ground level (mean of minimum and maximum monthly temperatures over 1972–2004, T-ESP, 2006).

2.2. Site selection and experimental design

In January 2005, near the start of the dry season, one large and one small natural gap were selected in undisturbed forest on the central plateau of BCI (Fig. 1). The gaps were chosen because of their relatively flat local relief, freely draining soil, absence of gullies and streams, and proximity to the Forest Dynamics Plot 1 km to the east (Fig. 1), with which they share the same soil type (Ava, a red light clay, Baillie et al., 2007) and andesite parent material (Johnsson and Stallard, 1989; Baillie et al., 2007). The small and large gaps were 10 and 565 m² (following the definition of Brokaw, 1982), 190 and 820 m² (definition of van der Meer and Bongers, 1996) or 310 and 1040 m² in size (Runkle’s definition, as modified in van der Meer et al., 1994). Part of the crown of a dead tree was removed from the large gap (without disturbance) because it was covering the only sapling-free area.

Three 2 m \times 2 m plots (separated by >50 cm) were marked out in a relatively vegetation-free central area of both gaps and any remaining ground vegetation was cut and removed without disturbing the natural soil and litter conditions. The treatments were (a) TRENCHED: in which a 25 cm wide trench 20 cm deep was dug around the outside of the plot, lined with a plastic sheet and refilled, (b) CLEARED: in which all litter was removed, and (c) CONTROL. Litter was not measured during the experiment, but in July 2005 the mean dry mass of litter in the same gaps was 0.873 ± 0.113 kg/m² (mean \pm S.E., $n = 12$ samples of area 78.5 cm² each) with no significant dif-

ference between the two gaps (unpaired *t*-test, $n_1 = n_2 = 6$, $p = 0.224$).

The experiment was carried out during the dry season of 2004/2005, during two separate periods. Measurements were initiated in the large gap on 7 February 2005 and in the small gap on 8 March, just after each plot had been irrigated by watering can with 30 mm of water (with no runoff). Since 23 mm of rain fell between 01:15 and 06:00 h on 9 February and effectively re-irrigated the large gap, the start time was re-set to 06:00 h on 9 February for this experiment.

Meteorological measurements were taken close to the centre of both gaps for 17 days using a MiniMET station at a height of 1.15 m with the net radiometer centered above the control plot. Air temperature, relative humidity, net radiation (Monteith and Unsworth, 1990) and wind speed were logged automatically at 10 min intervals (the anemometer was a Kleinwindgeber from A. Thies GmbH & Co. KG, Göttingen, Germany, and all other equipment was from Skye Instruments Ltd., Llandrindod Wells, UK). Soil temperature at 5 and 50 mm depth was recorded at the same time intervals in the control plot using bead thermistors (two at each depth, on opposite sides of the plot) connected to a data logger (all equipment from Skye Instruments Ltd.).

After irrigation, soil matric potential was measured in each plot at 0–5, 5–10, 15–20 and 45–55 mm depths using the filter-paper technique with a laboratory-calibrated batch of filter papers (Deka et al., 1995; Mullins, 2001) between 09:00 and 11:45 h on all days except weekends. Thin layers of soil were excavated using a 10 cm wide straight-edged scraper that was sharpened to cut through roots and bent to facilitate removal of a horizontal layer from above. This was pushed at a constant depth up against a flat metal surface scribed with horizontal lines at the relevant depths.

Although both the large and small gap experiments were carried out in the dry season, conditions differed slightly between the two periods. During the large gap experiment,

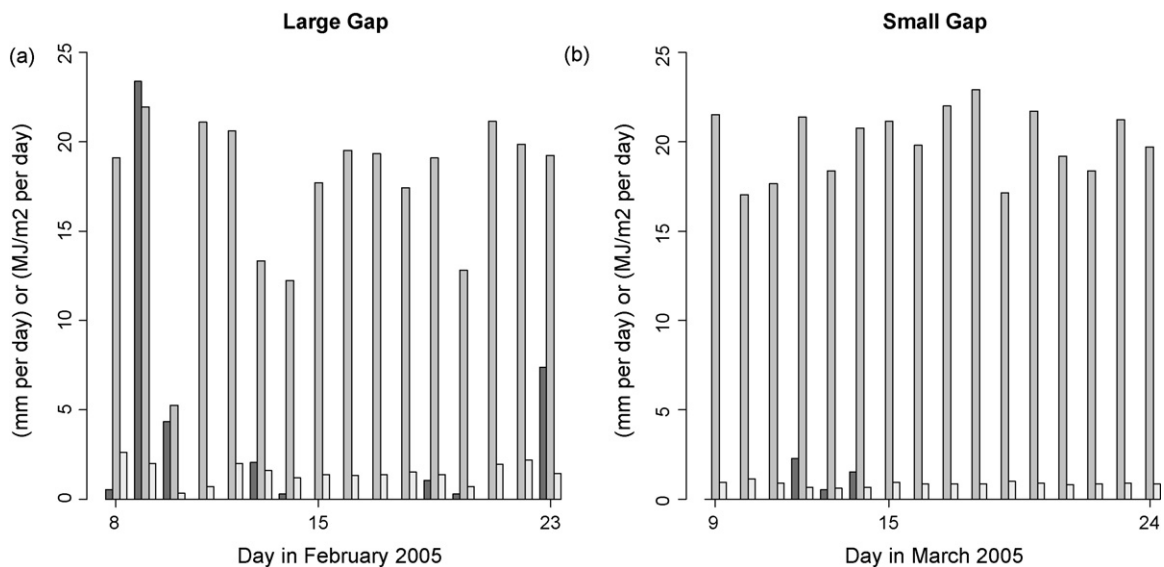


Fig. 2 – Rainfall, above-canopy solar radiation and within-gap net radiation (left to right) during the two experiments (a: large gap and b: small gap; measured in 5 min periods and converted to daily totals). Only days of complete data shown (i.e. 7 February and 8 March excluded).

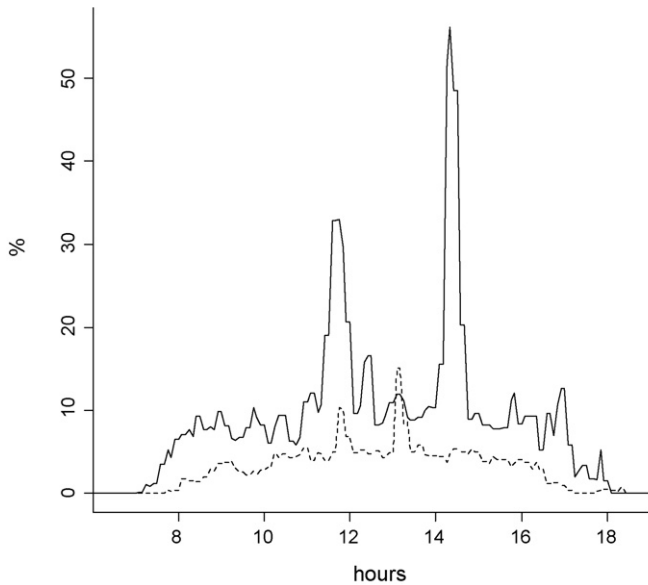


Fig. 3 – The mean daily radiation regime in the large (solid line) and small (broken line) gaps for 06:30–18:30 h, showing within-gap net radiation expressed as a percentage of above-canopy solar radiation recorded at 48 m height on the Lutz Tower on BCI. The mean is taken over all complete days for each experiment, but variability was high between days, ranging over approximately a factor of two higher or lower at any particular time (not shown). Sunrise and sunset times during the large gap experiment were 06:41 and 18:26 h, and for the small gap experiment were 06:29 and 18:27 h.

rainfall averaged 0.58 mm/day with 57.1% of days receiving no rain, whilst in the small gap experiment rainfall averaged 0.28 mm/day with 77.8% of days receiving no rain (Fig. 2). Total daily net radiation in the large gap averaged 1.48 MJ/m² per day (8.45% of total above-canopy solar radiation) and the small gap averaged 0.85 MJ/m² per day (4.25%) (Figs. 2 and 3). Only the large gap received >25% of solar radiation at ground level and only for an average of 40 min per day (11:35–11:55 and 14:15–14:35 h, Fig. 3). During the large gap experiment, the sky was consistently partly to mostly cloudy, whereas during the small gap experiment the sky was clearer. Above-canopy mean air temperature was 25.2 °C during the large gap experiment and 26.2 °C during the small gap experiment, with air temperature in the gaps themselves slightly lower at 25.0 and 25.9 °C, respectively. Within-gap wind speed was <1 m/s 76.3% of the time overall (including night hours), but speeds up to 11.4 m/s (large gap) and 7.4 m/s (small gap) occurred during the day.

2.3. The SWEAT model

The transport model Soil Water Energy and Transpiration (SWEAT), Daamen and Simmonds, 1994, 1996; Daamen, 1997) uses meteorological data, vegetation and soil parameters and initial profile values of soil temperature, T (in °C), and soil matric potential, ψ (soil water availability in kPa, always ≤ 0 ;

Mullins, 2001), to simulate water and heat flow in soil and hence to predict future values of soil T and ψ at a range of depths. SWEAT models soil heat and water flow as a coupled process, so that water vapour transfer (mainly controlled by T gradients) and water movement (mainly controlled by ψ gradients) are more reliably predicted, which greatly improves simulation accuracy in the top 50 mm of the soil (Daamen and Simmonds, 1994).

SWEAT uses a boundary layer approach (Monteith and Unsworth, 1990) modified from Choudhury and Monteith (1988), dividing the soil-vegetation environment into three layers: (1) AIR between the height where meteorological readings are taken (reference height) and either the top of the soil profile (if no vegetation is present) or the zero plane displacement height (the height at which all aerodynamic shearing stresses due to the presence of vegetation are assumed to act, Monteith and Unsworth, 1990), (2) SUBCANOPY (if vegetation is present) between the zero plane and the top of the soil profile and (3) SOIL, being the soil profile down to either an impermeable or a freely draining depth (usually 2–3 m), which may be further divided into soil layers. SWEAT does not model litter as a separate layer: the soil profile ends at the top of the mineral horizon and the physical influence of litter, if present, is modelled by scaling heat and vapour fluxes at the surface boundary, which is an adequate approach in this situation.

SWEAT versions 1.0–3.0.3 were written in Turbo Pascal (Borland® International). In order to solve compilation and compatibility problems encountered in this study, version 3.0.3 was re-written in R (a GNU® freeware language, R Development Core Team, 2006) with improved input and output routines (version 5.2, <http://www.abdn.ac.uk/sweat>). The physics and controlling equations behind this model were not changed during re-writing apart from modifications described in the next section.

2.4. Modelling the soil water characteristic

To simulate movement of soil water, SWEAT uses a standard model based on Darcy's law (Marshall et al., 1996), referred to here as Campbell's model (Campbell, 1974, 1985; Shao and Irannejad, 1999). In this model, the relationships between θ (the proportion by volume of water in the soil), k (soil hydraulic conductivity in cm/s) and ψ (in kPa) are given by the following equations (Brooks and Corey, 1964; Campbell, 1985: Eqs. (5.9) and (6.14)):

$$\theta = \begin{cases} \theta_{\text{sat}} & \text{for } \psi \geq \psi_e \\ \theta_{\text{sat}} \left(\frac{\psi}{\psi_e} \right)^{-1/b} & \text{for } \psi < \psi_e \end{cases} \quad (1)$$

$$k = \begin{cases} k_{\text{sat}} & \text{for } \psi \geq \psi_e \\ k_{\text{sat}} \left(\frac{\psi}{\psi_e} \right)^{-2-3/b} & \text{for } \psi < \psi_e \end{cases} \quad (2)$$

where θ_{sat} and k_{sat} are the values of θ and k when the soil is saturated (i.e. all soil pores are water-filled), ψ_e the air-entry potential (a potential defined in Campbell's model so that for $\psi \geq \psi_e$ (i.e. $|\psi| \leq |\psi_e|$) the soil is assumed to be saturated, Shao

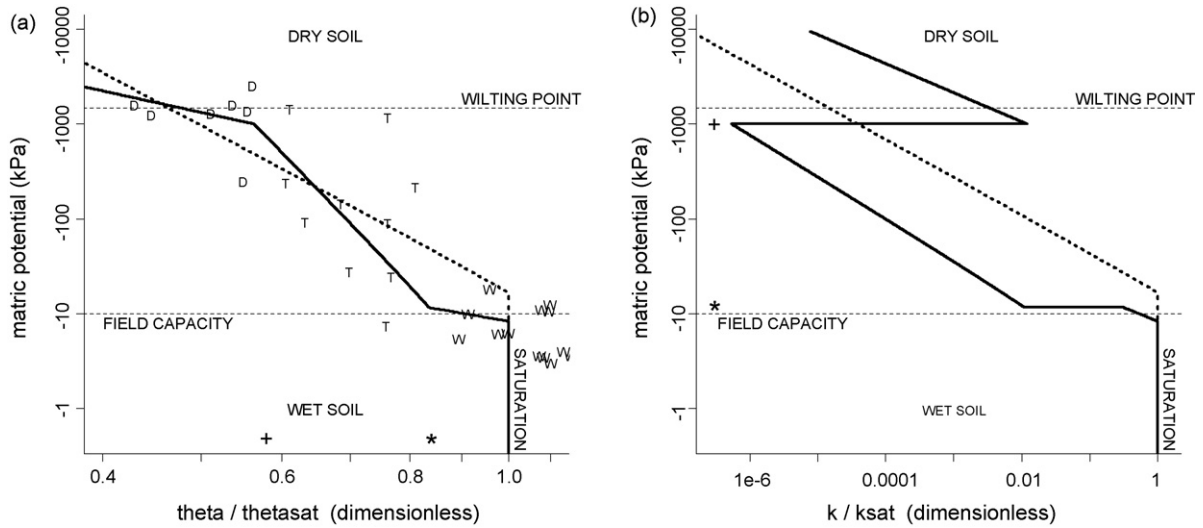


Fig. 4 – (a) An example soil water characteristic. Data points (D, T, W) are taken from the small gap at 5–10 mm depth ($\theta_{\text{sat}} = 0.69 \text{ cm}^3/\text{cm}^3$, $k_{\text{sat}} = 0.001 \text{ cm/s}$). The broken line shows the fit to Campbell’s model (Eq. (1)) from a linear regression on all data points (Eq. (3)). The solid line shows a three-sticks fit where regressions on the dry (D) and wet (W) points are calculated separately and then bridged by a straight line covering transitional values (T; for + and * see text). (b) The relationship between ψ and k implied by (a) and Eq. (2) (broken line, Campbell’s; solid line, three-sticks; in this example the diagonal section of the solid line between + and * is slightly steeper, and the other two diagonal sections are less steep, than the broken line).

and Irannejad, 1999) and b is a dimensionless factor. For $\psi < \psi_e$, Eq. (1) is equivalent to:

$$\log_{10}(\psi) = -b \log_{10} \left(\frac{\theta}{\theta_{\text{sat}}} \right) + \log_{10}(\psi_e) \quad (3)$$

Thus, in Campbell’s model the soil water characteristic (the relationship between ψ and θ , Townend et al., 2001) is completely described by parameters b and ψ_e (Eq. (1)), obtained from a regression (on log–log axes) on a set of ψ readings (it is more appropriate to use field data than laboratory data for this regression because of hysteresis, see Mullins, 2001; Townend et al., 2001).

The soil water characteristic is important for reliable modelling of the soil water regime because it is used to relate ψ and θ during the simulation (Eq. (1)) and the same parameters are used to derive k (Eq. (2)). Although Campbell’s model, which describes a broad, unimodal soil pore size distribution, is a good fit to many soils, it was found to be a poor fit to soil on BCI at <100 mm depth. Measurements of ψ and θ at <55 mm depth showed clear evidence of a predominantly bimodal pore size distribution (Childs, 1969, e.g. Fig. 4), which corresponded to the observed aggregation of the soil at these depths, with structural pores between the aggregates (corresponding to the W points in Fig. 4a) and textural pores within the aggregates. Consequently, it was impossible to fit model outputs to field observations without using a function that was a better fit to the soil water characteristic. At 0–100 mm depths, a three-sticks fit was used instead of Campbell’s model to describe the soil water characteristic (points were designated dry, wet or transitional (T) according to two threshold water contents $\theta_+ = (0.3940 - 0.0008 \times D) \text{ cm}^3/\text{cm}^3$ and

$\theta_* = (0.5945 - 0.0025 \times D) \text{ cm}^3/\text{cm}^3$ (D = depth in mm), marked + and * in Fig. 4, chosen empirically from consideration of the shapes of all characteristics measured). At >100 mm depth, a fit was derived from ψ and θ data from a separate study in this area of BCI (Mullins et al., unpublished data) which fitted Campbell’s model acceptably well. The three-stick fitting procedure caused two unrealistic discontinuities in the relationship between ψ and k (+ and *, Fig. 4b), but was acceptable for our purposes because it gave an improved representation of k_{unsat} and the water characteristic in soil close to saturation (where most water moves) in comparison to Campbell’s model. Furthermore, since SWEAT’s ψ output was insensitive to the value of k_{sat} at all depths (see below), capillary flux made a much smaller contribution to changes in the water content of the 0–100 mm depth layer than atmospheric drying and the predicted water fluxes at the surface and 100 mm depth will have been reliable. Unrealistically small values of k_{unsat} at a few points at some depths during the simulation were avoided by restricting k_{unsat} within SWEAT to $\geq 10^{-10} \text{ cm/s}$.

2.5. Calibrating the model

The input parameters required to run SWEAT were collected from measurements where possible, and otherwise estimated from literature (Table 1). However, SWEAT also requires a calibration stage to set the values of k_{sat} (Fig. 4) and four other inputs: a multiplier for total soil thermal conductivity, m_{tk} (multiplies $(\lambda_{\text{T}})_{\text{soil}}$ in Daamen and Simmonds, 1994:Eq. (2.14)), a multiplier for the thermal conductivity of dry soil, $m_{\text{dry tk}}$ (multiplies D in Daamen and Simmonds, 1994:Eq. (2.14)), a multiplier for the resistance to heat and vapour flux in the

Table 1 – Input parameters and required by the SWEAT model for a gap simulation

Input parameter	Values																		
Meteorological data	From MiniMET data (converted from 10 min to 5 min values by interpolation)																		
Simulation start times	Large gap on Julian day 40 (9 February) at 06:00 (21600 s after midnight), small gap on day 67 (8 March) at 13:40 (49200 s)																		
Radiation	Net																		
Reference height (z_u)	1.15 m (see Methods)																		
Soil layers	25 layers down to 3 m (node depths (mm): 2.5, 7.5, 12.5, 17.5, 22.5, 27.5, 32.5, 37.5, 42.5, 47.5, 52.5, 57.5, 62.5, 67.5, 72.5, 127.5, 172.5, 227.5, 272.5, 527.5, 872.5, 1127.5, 1872.5, 2127.5, 2872.5, 3127.5) and the soil profile was freely draining (Baillie et al. 2007).																		
Leaf Area Index (LAI)	0 m ² /m ² (with no 'extra LAI', Daamen and Simmonds 1994)																		
Substrate roughness height (z_0^s)	0.01 m without litter; 0.05 m with litter (T. Marthews pers. obs., 2005)																		
Initial soil temperature (T)	22.4°C and 23.7°C for the large gap and 26.0°C and 25.3°C for the small gap, at 0–45 mm and 45–3000 mm respectively (average of the initial temperatures in the control plot).																		
Initial soil matric potential (ψ)	As wet as SWEAT allows at all depths (large gap -10 kPa, small -15 kPa [*]) except at 700–2000 mm depth where $\psi = -1000$ kPa was assumed [†] .																		
Soil clay (f_c) and quartz fractions	0.38 and 0.33 at all depths, respectively (Becker et al. 1988, cf. Yavitt 2000)																		
Soil dry bulk density (and θ_{sat})	0.83 g/cm ³ (≤ 70 mm depth) and 0.95 g/cm ³ (> 70 mm) (Sayer et al. 2006, cf. Cavelier 1992, Yavitt 2000) ^{**}																		
b and ψ_e	These are the values obtained from regressions (eqn. 3, Fig. 4) on the ψ data (L = large gap, S = small gap, W = wet end regression, D = dry end, all ψ_e values in kPa) ^{††} .																		
	<table border="1"> <thead> <tr> <th></th> <th>0–5 mm depth</th> <th>5–15 mm</th> <th>15–45 mm</th> <th>45–100 mm</th> <th>100–3000 mm</th> </tr> </thead> <tbody> <tr> <td>L</td> <td>W: $b=2.2$, $\psi_e=-5$ D: $b=2.6$, $\psi_e=-404$</td> <td>W: $b=1.7$, $\psi_e=-4$ D: $b=6.0$, $\psi_e=-20$</td> <td>W: $b=1.3$, $\psi_e=-5$ D: $b=2.8$, $\psi_e=-233$</td> <td>W: $b=2.4$, $\psi_e=-3$ D: $b=5.7$, $\psi_e=-14$</td> <td>$b=14.5$, $\psi_e=-1$</td> </tr> <tr> <td>S</td> <td>W: $b=3.0$, $\psi_e=-10$ D: $b=4.1$, $\psi_e=-93$</td> <td>W: $b=1.7$, $\psi_e=9$ D: $b=2.4$, $\psi_e=-261$</td> <td>W: $b=3.6$, $\psi_e=8$ D: $b=0.8$, $\psi_e=-535$</td> <td>W: $b=3.3$, $\psi_e=3$ D: $b=9.2$, $\psi_e=-1.7$</td> <td></td> </tr> </tbody> </table>		0–5 mm depth	5–15 mm	15–45 mm	45–100 mm	100–3000 mm	L	W: $b=2.2$, $\psi_e=-5$ D: $b=2.6$, $\psi_e=-404$	W: $b=1.7$, $\psi_e=-4$ D: $b=6.0$, $\psi_e=-20$	W: $b=1.3$, $\psi_e=-5$ D: $b=2.8$, $\psi_e=-233$	W: $b=2.4$, $\psi_e=-3$ D: $b=5.7$, $\psi_e=-14$	$b=14.5$, $\psi_e=-1$	S	W: $b=3.0$, $\psi_e=-10$ D: $b=4.1$, $\psi_e=-93$	W: $b=1.7$, $\psi_e=9$ D: $b=2.4$, $\psi_e=-261$	W: $b=3.6$, $\psi_e=8$ D: $b=0.8$, $\psi_e=-535$	W: $b=3.3$, $\psi_e=3$ D: $b=9.2$, $\psi_e=-1.7$	
	0–5 mm depth	5–15 mm	15–45 mm	45–100 mm	100–3000 mm														
L	W: $b=2.2$, $\psi_e=-5$ D: $b=2.6$, $\psi_e=-404$	W: $b=1.7$, $\psi_e=-4$ D: $b=6.0$, $\psi_e=-20$	W: $b=1.3$, $\psi_e=-5$ D: $b=2.8$, $\psi_e=-233$	W: $b=2.4$, $\psi_e=-3$ D: $b=5.7$, $\psi_e=-14$	$b=14.5$, $\psi_e=-1$														
S	W: $b=3.0$, $\psi_e=-10$ D: $b=4.1$, $\psi_e=-93$	W: $b=1.7$, $\psi_e=9$ D: $b=2.4$, $\psi_e=-261$	W: $b=3.6$, $\psi_e=8$ D: $b=0.8$, $\psi_e=-535$	W: $b=3.3$, $\psi_e=3$ D: $b=9.2$, $\psi_e=-1.7$															

Symbols in the first column are from Daamen and Simmonds (1994).

*Initial values less negative than these were found to overload SWEAT's method of simulating ponding (Daamen and Simmonds, 1994) so the measured initial values (Figs. 5 and 7) were not used.

**SWEAT uses a set density of soil solids of 2.65 g/cm³ and derives the value of θ_{sat} from $\theta_{sat} = 1 - (\text{dry bulk density}/2.65)$ (Marshall et al., 1996:Eq. (1.4)).

†The initial amount of rainfall and irrigation in both experiments penetrated to 700 mm (supported by readings taken nearby on 27 January and 10 February, Mullins et al., unpublished data) and conditions were assumed to be dry below this to 2 m depth, below which the low root density and proximity to a paralithic surface at 3.5 m (Baillie et al., 2007) implied the soil was again wet.

††It is not important that the dry end values of ψ_e are out of the usual range for this quantity (Campbell, 1985:46) because they are not used when the soil is very wet.

air layer just above the soil surface, m_r (if there is no vegetation this multiplies the air layer resistance r_a , Choudhury and Monteith, 1988, otherwise it multiplies the subcanopy layer aerodynamic resistance r_{scan} , Daamen, 1997) and a multiplier for thermally-driven soil vapour flow, m_η (multiplies the vapour flow enhancement factor η , Campbell, 1985; Parlange et al., 1998; Grifoll et al., 2005). Additionally, the multiplier m_r took different values for bare and littered soil, denoted here m_{rb} and m_{rl} , respectively (litter not modelled as part of the soil layer). k_{sat} was obtained through calibration rather than measurement because of its high variability in the field and the difficulty of obtaining a representative value (van Genuchten, 1980; Marshall et al., 1996; Dirksen, 2001).

Since the results of SWEAT in all runs were unaffected by the values of the two multipliers for thermal conductivity (m_{tk} and $m_{dry tk}$), these were set to the default value of 1, leaving

four calibration values (k_{sat} , m_{rb} , m_{rl} and m_η) to be determined in four steps:

- (1) The first calibration step was to establish the bounds within which SWEAT would complete its simulations, which were controlled by k_{sat} . Exhaustive runs of SWEAT established that it would complete only with k_{sat} values in the range $3-10 \times 10^{-4}$ cm/s at 0–30 mm depth and $3-20 \times 10^{-5}$ cm/s at 30–3000 mm, but that the outputs were not sensitive to k_{sat} within this range, therefore profile values of k_{sat} were chosen within these bounds. The values 0.001 cm/s (0–30 mm) and 0.0001 cm/s (30–3000 mm) were used, which are appropriate for a clay soil with a finely aggregated upper layer (Marshall et al., 1996:Table 4.1).
- (2) Matching the matric potential output on a large gap run (i.e. no vegetation) without litter against measured values

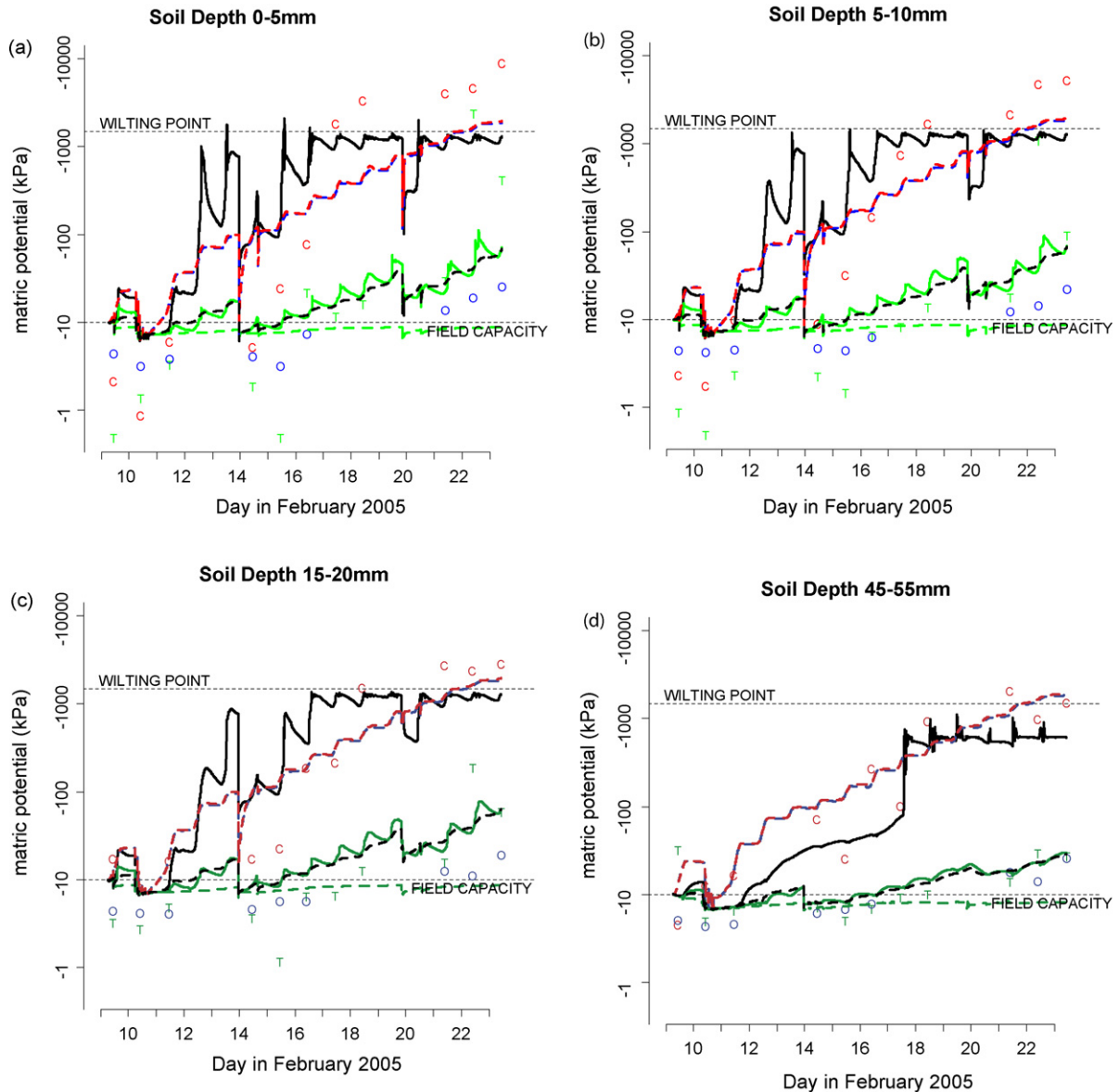


Fig. 5 – Matric potentials in the large gap. (a) Soil depth: 0–5 mm; (b) soil depth: 5–10 mm; (c) soil depth: 15–20 mm; (d) soil depth: 45–55 mm. Points indicate readings from the TRENCHED (T), CLEARED (C) and CONTROL (O) plots. Solid lines indicate trenched (blue [lower on the black-and-white version of this figure]) and trenched + cleared (red [upper on the black-and-white version of this figure]) gap simulations. Broken lines indicate trenched (lowest), trenched + cleared (low), cleared and control (last two highest and closely similar) understorey simulations. Initial simulated value set to -10 kPa to avoid ponding (q.v. Table 1). Tick marks denote midnight at the start of the day. (For interpretation of the references to color in this figure legend, the reader is referred to the web version of the article.)

from the cleared plot (where soil drying would have been the most intense) was used to set the value of m_{rb} . The optimal value was $m_{rb} = 0.85$ (i.e. the actual resistance r_a was 15% lower than the resistance above bare soil assumed by SWEAT, probably just indicating that the mean substrate roughness height was slightly less than the estimate of 1 cm made in the field, Table 1). This and calibration step 4 required the assumption that water extraction by surrounding forest roots (not modelled in SWEAT) had little effect on the rate of soil drying, which was justified by the close similarity between the control and trenched

matric potential and temperature readings in the large gap (Figs. 5 and 6 excluding two dry readings from the trenched plot at 5 mm depth which were taken to be outliers).

- (3) Matching the matric potential output on a large gap run with litter against measured values from the trenched plot was used to set the value of m_{rl} . The optimal value was $m_{rl} = 50$ (i.e. the effect of litter in the gap was to increase aerodynamic resistance above the soil surface by a factor of $(50/0.85) = 58.8$).
- (4) Matching the temperature output on a large gap run with litter against measured values from the control plot

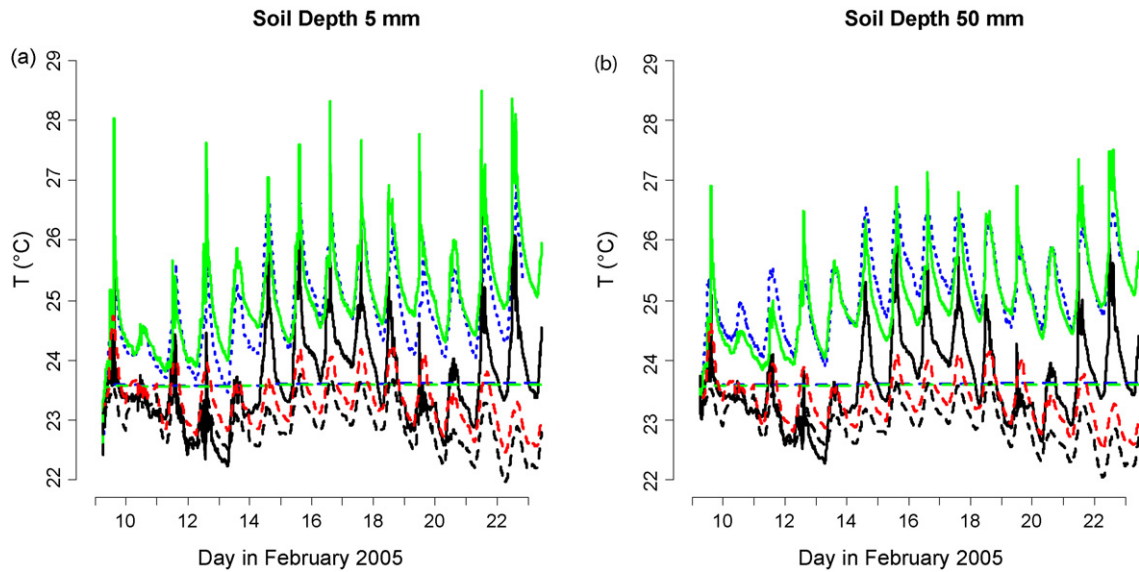


Fig. 6 – Temperatures in the large gap. (a) Soil depth: 5 mm; (b) soil depth: 50 mm. The dotted line indicates readings from the control plot (average of two replicate measurements, mean difference 0.35 °C). Solid lines indicate trenched (red [upper on the black-and-white version of this figure]) and trenched + cleared (blue [lower on the black-and-white version of this figure]) gap simulations. Broken lines indicate trenched + cleared (lowest), cleared (low), trenched and control (last two horizontal and closely similar) understory simulations. Tick marks denote midnight at the start of the day. (For interpretation of the references to color in this figure legend, the reader is referred to the web version of the article.)

Table 2 – Summary of all measurements (points) in Figs. 5a, 5d, 6, 7a, 7d and 8

	T in °C		Soil drying	
	5 mm depth	50 mm	5 mm	50 mm
Large gap				
Control	24.8 ± 1.0	25.2 ± 0.8	Still wet after 14 days	Still wet after 14 days
Trenched			Dry after 14 days	Still wet after 14 days
Cleared			Very dry after 8–9 days	Very dry after 10–12 days
Small gap				
Control	25.7 ± 1.4	25.6 ± 0.7	Very dry after 10–11 days	Very dry after 9–10 days
Trenched			Still wet after 16 days	Still wet after 16 days
Cleared			Very dry after 8–9 days	Very dry after 10–11 days

Temperatures are mean ± mean diel range (only measured in the control plot). For soil drying, wet means $\psi > -50$ kPa, fairly dry means $-50 > \psi > -300$ kPa, dry means $-300 > \psi > -1500$ kPa and very dry means $\psi < -1500$ kPa.

Table 3 – Summary of all simulations of the large and small gaps (large gap results were used for calibration) in Figs. 5a, 5d, 6, 7a, 7d and 8

	T in °C		Soil drying	
	5 mm depth	50 mm	5 mm	50 mm
Large gap				
Trenched	25.0 ± 1.4	25.0 ± 1.0	Fairly dry after 14 days	Still wet after 14 days
Trenched + cleared	23.6 ± 1.2	23.6 ± 0.9	Dry after 4–5 days	Dry after 8 days
Small gap				
Trenched	26.2 ± 0.5	26.1 ± 0.3	Still wet after 16 days	Still wet after 16 days
Trenched + cleared	24.8 ± 0.6	24.8 ± 0.5	Dry after 12 days	Dry after 15 days

Temperatures are mean ± mean diel range. For soil drying, wet means $\psi > -50$ kPa, fairly dry means $-50 > \psi > -300$ kPa, dry means $-300 > \psi > -1500$ kPa and very dry means $\psi < -1500$ kPa.

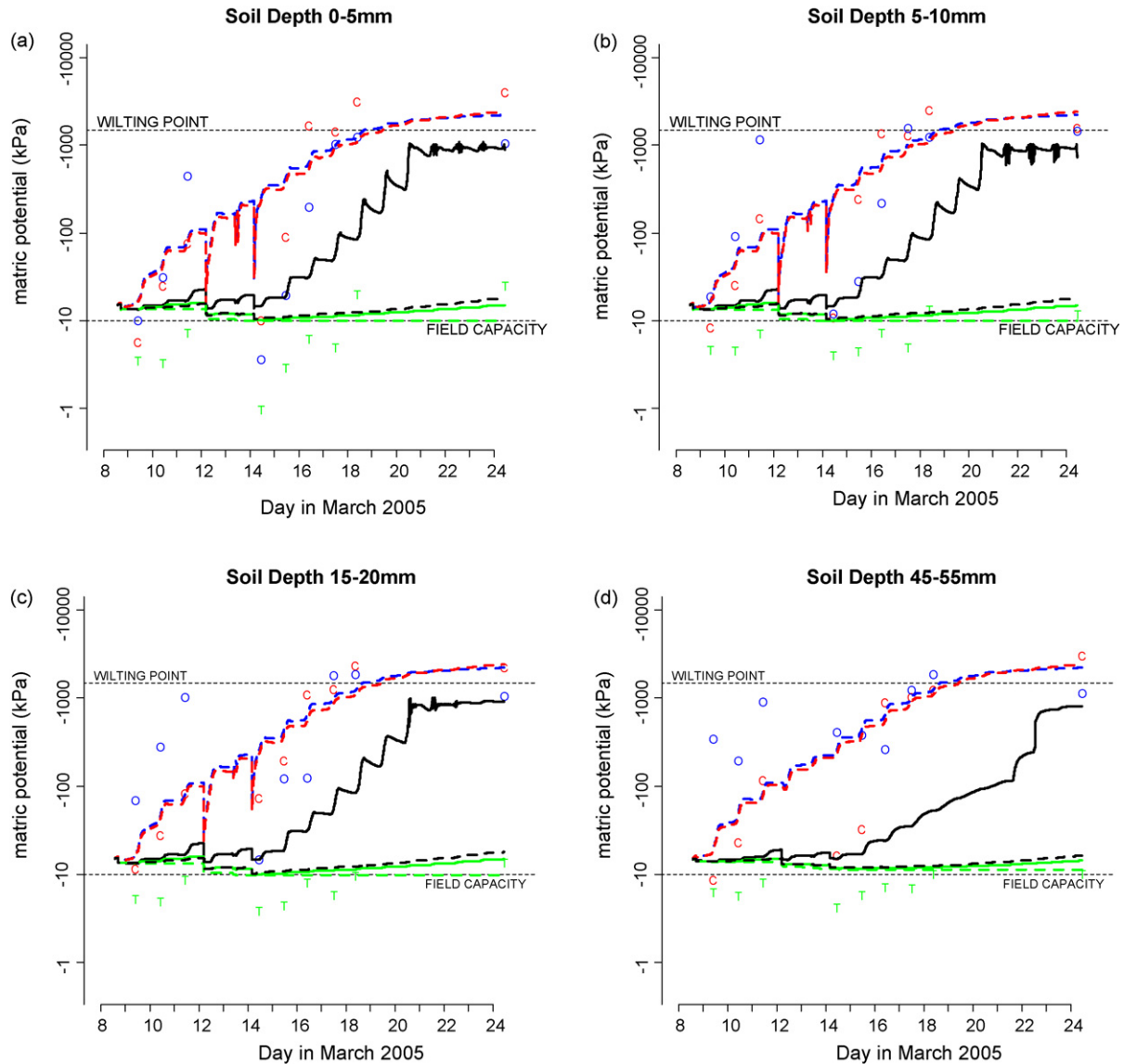


Fig. 7 – Matric potentials in the small gap. (a) Soil depth: 0–5 mm; (b) soil depth: 5–10 mm; (c) soil depth: 15–20 mm; (d) soil depth: 45–55 mm. Points indicate readings from the trenched (T), cleared (C) and control (O) plots. Solid lines indicate trenched (blue [lower on the black-and-white version of this figure]) and trenched + cleared (red [upper on the black-and-white version of this figure]) gap simulations. Broken lines indicate trenched (lowest), trenched + cleared (low), cleared and control (last two highest and closely similar) understorey simulations. Initial simulated value set to –15 kPa to avoid ponding (q.v. Table 1). Tick marks denote midnight at the start of the day. (For interpretation of the references to color in this figure legend, the reader is referred to the web version of the article.)

was used to set the value of m_η . The optimal value was $m_\eta = 200$ (i.e. thermally-driven vapour flow was increased by a factor of 200 in addition to the usual enhancement η calculated by SWEAT using the equations in Daamen and Simmonds, 1994).

After each calibration step, the preceding steps were repeated to check whether the optimal values were affected by later changes, but no interdependency was found between the four calibration parameters.

2.6. Model simulations

The large gap observations were used to calibrate SWEAT, and then the measurements from the trenched plot in the small gap were used for validation. Agreement with the ψ readings from the trenched plot in the small gap was very close at both 5 and 50mm depths, with the soil remaining wet ($\psi > -30$ kPa) at the end of the experiment according to both simulations and readings (Fig. 7; Tables 2 and 3).

SWEAT was used to make predictions for both gap environments and, additionally, simulations were carried out of a

Table 4 – Input parameters required by the SWEAT model for an understorey simulation

Input parameter	Values
Meteorological data	From T-ESP (2006) (converted from 15 to 5 min values by interpolation)
Simulation start times	As in Table 1
Radiation	Solar
Reference height (z_u)	48 m (the height of the Lutz tower on BCI)
Soil layers	As in Table 1
Leaf Area Index (LAI)	16.5 m ² /m ² (Jordan, 1993:Table 3), assumed 100% transpiring (with no 'extra LAI')
Canopy (crop) height (h)	30 m
Radiation transmission coefficient (A_c)	0.7 (Monteith and Unsworth, 1990:Table 5.1)
Crop average leaf width (w)	0.05 m (SWEAT default)
(ψ_{critical}) and the exponent of $\psi_{\text{leaf}}/\psi_{\text{critical}}$ (Y)	$\psi_{\text{critical}} = -1600$ kPa and $Y = 20$ (Campbell, 1985:Eq. (12.28))
Vegetation albedo	0.20 (Monteith and Unsworth, 1990:Table 6.1)
Substrate roughness height (z_0^s)	As in Table 1
Initial soil temperature (T)	As in Table 1
Initial soil matric potential (ψ)	As in Table 1
Root density	Total root length of 250 km/m ² was distributed** in the layers 0–50, 50–100, 100–150, 150–200, 200–250, 250–700 and 250–3000 mm according to the ratios 100:74:65:59:37:4:0
Soil clay (f_c) and quartz fractions	As in Table 1
Soil dry bulk density (and θ_{sat})	As in Table 1
b and ψ_e (q.v. Fig. 4)	As in Table 1

Symbols in the first column are from Daamen and Simmonds (1994).

* On the BCI 50 ha plot the average canopy height was 24.6 ± 9.5 m (2000 figures), but the distribution was far from normal with an overall mode at 29.5 m and secondary modes at 18 m and 40 m (Welden et al., 1991; Hubbell et al., 1999; S. Hubbell, L. Comita and R. Condit, unpublished data).

** Total root length was calculated from an estimate of 105 kg/m² (=94.5/0.90) for the Gigante forest (Cavelier, 1992) 1 km S of BCI, converted to a volume of wood assuming the average wood density of the BCI forest (540 kg/m³, Chave et al., 2003) and finally to a root length by assuming all roots are 1 mm in diameter (necessary for SWEAT). The distribution of roots down the soil profile was taken from Cavelier (1992)'s measurements on roots up to 50 mm diameter, assuming 10% of roots below 250 mm and no roots below 700 mm (Dietrich et al., 1982:Fig. 5).

virtual treatment plot in the understorey with the same initial conditions (irrigation) and supporting a 'crop' of forest trees (input parameters estimated from literature, Table 4). Since there was root water extraction from trees within this virtual plot, 'untrenched' simulations were possible in the understorey, although these simulations should be interpreted cautiously because SWEAT was originally designed for sparse vegetation only (Daamen, 1997) and this is its first use for LAI > 4 m²/m².

3. Results

3.1. Soil drying

In the small gap, soil drying in both untrenched plots was sufficient to dry the soil profile to 50 mm depth from field capacity to permanent wilting point in 8–11 days whether or not litter was present, whilst soil from the trenched plot remained

Table 5 – Summary of all simulations of the understorey in Figs. 5a, 5d, 6, 7a, 7d and 8

	T in °C		Soil drying	
	5 mm depth	50 mm	5 mm	50 mm
In February 2005				
Control	23.6	23.6	Very dry after 12–13 days	Very dry after 12–13 days
Trenched	23.6	23.6	Still wet after 14 days	Still wet after 14 days
Cleared	23.3 ± 0.4	23.3 ± 0.4	Very dry after 12–13 days	Very dry after 12–13 days
Trenched + cleared	22.9 ± 0.4	22.9 ± 0.4	Fairly dry after 14 days	Still wet after 14 days
In March				
Control	25.4	25.4	Very dry after 10–11 days	Very dry after 10–11 days
Trenched	25.4	25.4	Still wet after 16 days	Still wet after 16 days
Cleared	24.5 ± 0.3	24.5 ± 0.3	Very dry after 10–11 days	Very dry after 10–11 days
Trenched + cleared	24.2 ± 0.3	24.2 ± 0.3	Still wet after 16 days	Still wet after 16 days

Temperatures are mean ± mean diel range. For soil drying, wet means $\psi > -50$ kPa, fairly dry means $-50 > \psi > -300$ kPa, dry means $-300 > \psi > -1500$ kPa and very dry means $\psi < -1500$ kPa.

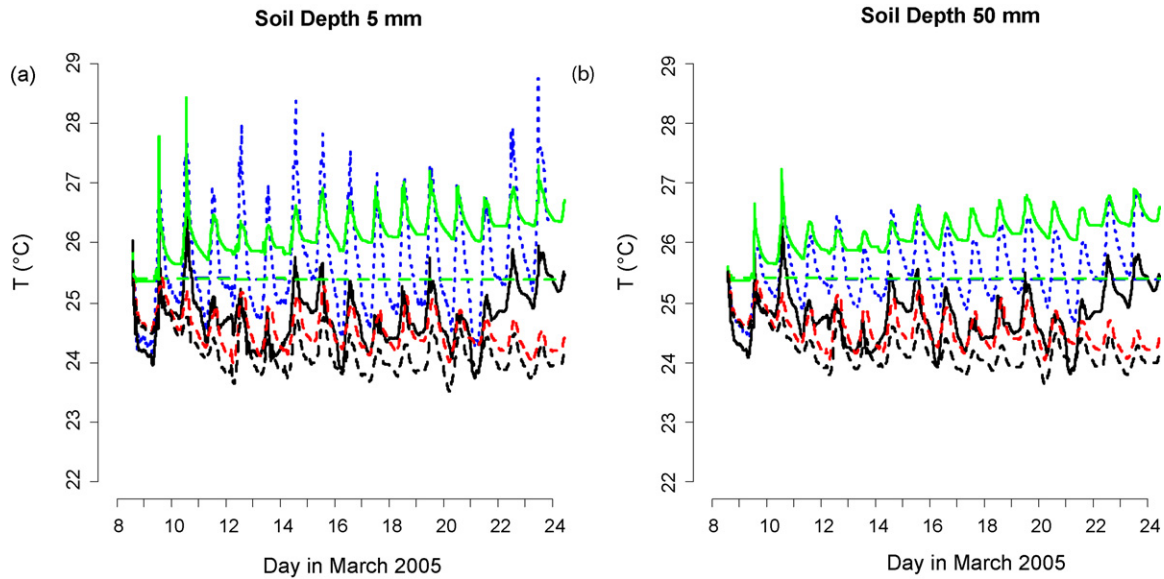


Fig. 8 – Temperatures in the small gap. (a) Soil depth: 5 mm; (b) soil depth: 50 mm. The dotted line indicates readings from the control plot (average of two replicate measurements, mean difference 0.35 °C). Solid lines indicate trenched (red [upper on the black-and-white version of this figure]) and trenched + cleared (blue [lower on the black-and-white version of this figure]) gap simulations. Broken lines indicate trenched + cleared (lowest), cleared (low), trenched and control (last two horizontal and closely similar) understorey simulations. Tick marks denote midnight at the start of the day. (For interpretation of the references to color in this figure legend, the reader is referred to the web version of the article.)

wet ($\psi = -15$ kPa) at both depths at the end of the experiment (Fig. 7; Table 2). This demonstrates that root water extraction was the dominant drying process. In the large gap, however, the cleared plot dried fastest, reaching wilting point to 50 mm depth within 8–12 days (Fig. 5; Table 2). Surface soil in the trenched plot dried slowly, approaching wilting point in 14 days, but deeper soil there and the soil profile to 50 mm in the control plot dried only slightly (Fig. 5; Table 2). This indicates that evaporation, when litter was absent, was the dominant drying process in the large gap (i.e. roots from the surrounding forest were either dead or absent, at least near the surface).

In the understorey, where root water extraction was simulated, SWEAT predicted that all untrenched soil would become very dry ($\psi < -1500$ kPa) within 10–13 days and that all trenched soil would remain wet ($\psi > -30$ kPa) for the duration of the experiments in both February and March (Figs. 5 and 7; Table 5, except the February trenched + cleared simulation at 5 mm depth which was predicted to become fairly dry ($\psi = -80$ kPa) after 14 days). This contrast was similar to the measured effect of trenching on drying rate in the small gap (9–11 days, Fig. 7; Table 2) and much greater than the effect of trenching in the large gap (no difference, Fig. 5; Table 2). Therefore, drying by the roots of surrounding trees was the dominant drying process in both the small gap and the understorey.

3.2. Soil temperature

The mean temperature of the control plot soil at 5 mm was 0.2 °C below gap air temperature and 0.4–0.5 °C below mean air temperature at 48 m above the canopy for both the large and the small gap experiments (Table 2), with the mean diel variation similar between the two gaps at 0.7–1.4 °C. The high

rainfall during 9–13 February in the large gap experiment (Fig. 2) temporarily depressed soil temperature by approximately 1 °C (Fig. 6), but no other trend in temperature could be attributed with certainty to rainfall.

In the understorey simulations for the plots with litter intact, there was an initial rise in soil temperature at both 5 and 50 mm depths to a value within 0.1 °C of the initial temperature of the soil profile at depth (Table 1), and the soil remained at this temperature day and night (Figs. 6 and 8; Table 5). This implies that the constant soil temperature resulted directly from heat conduction from soil at depth. In the absence of litter, the temperature to 50 mm depth was predicted to be 0.3–1.2 °C lower, and the amplitude of diel oscillation to rise from 0 to 0.3–0.4 °C (Figs. 6 and 8; Table 5), indicating that some evaporation and sensible heat transfer was occurring, despite the lack of direct sunlight in the simulated understorey. The predicted drop in temperature due to litter-removal increased to 1.3–1.4 °C in the small gap, in line with the anticipated increase in evaporative drying, but did not increase further in the large gap (Table 3), presumably as a result of a balance between the cooling effect of increased evaporation and the heating effect of direct sunlight. However, the diel oscillation in soil temperature was predicted to rise to 0.3–0.6 °C in the small gap and 0.9–1.4 °C in the large gap in the presence or absence of litter (Figs. 6 and 8; Table 3).

4. Discussion

4.1. Soil drying

Since any fast drainage would have occurred within 48 h of irrigation, most drying of the freely drained soil would have

been caused by root water extraction and evaporation at the soil surface (Marshall et al., 1996). In the large gap, soil evaporation was the dominant process. In the small gap and in the understorey, however, soil evaporation by direct solar radiation was small compared to root water extraction, which was the dominant process (Veenendaal et al., 1996; Poorter and Hayashida-Oliver, 2000). Therefore, gap size controlled soil drying by dictating the balance between root water extraction and soil surface evaporation. In general, there will be a moderate gap size in which both processes contribute substantially to drying, although this size will depend on how gap orientation and season control the proportion of direct solar radiation that is received.

Engelbrecht et al. (2001, 2006) found that bare soil in 225 m² gaps on the Buena Vista peninsula (<1 km from BCI) at 5–10 mm depth could dry to wilting point after 6 days of little or no rain (reported as “2 days after treatment start” and after “3 days of drought”, but this observation actually concerned soil drying 6 days after heavy (35.6 mm) rain on 6 July 2000 followed by light (5.3 mm) rain on 7 July and five rain-free (<0.3 mm) days, T-ESP, 2006). This is slightly faster than the 8–12 days observed for bare soil in our large gap (Fig. 5; Table 2), which is probably due to the observations having been made in July (when the days are longest) and on a different soil type (with a different pore size distribution).

These results are representative for small and large gaps on this soil type and time period because previous work on BCI has shown that replicated soil ψ measurements on a single soil type and topographic position yield results with limited scatter and a consistent drying behaviour (Daws et al., 2002; Mullins et al., unpublished data). Thus, the large within-gap differences in ψ between the plots are dominantly due to treatment effects as opposed to variability and measurement error. For comparison, at depths below 200 mm soil dries much more slowly, taking 30 days to dry from field capacity to wilting point during the dry season on BCI (Mullins et al., unpublished data; cf. 5–16 weeks recorded by Rand and Rand, 1982; Becker et al., 1988; Wright and Cornejo, 1990b; Veenendaal et al., 1996).

4.2. Soil temperature

Diel fluctuations in the soil temperature are caused by direct soil heating by the sun and/or sensible heat transfer during the day and cooling at night (on BCI, seasonal oscillations in temperature are only of the order of a few degrees) or the cooling effect of evaporation from the soil surface (Marshall et al., 1996). The increase in this oscillation with increasing gap size predicted by SWEAT concurs with the results of Pearson et al. (2002), and was unaffected by litter (although litter suppresses evaporation, it is attached to and has good thermal contact with the soil and therefore does not suppress heat flow).

For soil temperature in gaps, evaporation from bare soil is significant but direct solar heating is the dominant process (producing a strong diel oscillation), whereas in the understorey direct sunlight is generally cut off and evaporation, although reduced in comparison to the rate in gaps, becomes the dominant process. In gaps, evaporation in the absence of litter reduces the soil temperature in comparison to soil under litter both directly, through loss of latent heat, and indirectly, by increasing the overnight drop in temperature (drier

soil cannot conduct heat as effectively from the underlying soil).

4.3. Influence of litter

When litter was present in the large gap, aerodynamic resistance in the air directly above the soil (which includes the litter layer in SWEAT) increased by a factor of (m_{r1}/m_{rb})=58.8. When Mullins et al. (1996) used SWEAT to model the application of a straw mulch under an agricultural crop in the semi-arid tropics, they estimated (m_{r1}/m_{rb})=2, so the forest litter in the large gap apparently inhibited heat flow and vapour flow by an additional factor of 30. This large factor is reasonable for vapour flow (but not for heat flow) because the straw mulch consisted of a loose pile of mainly stalks (crop residue, Marshall et al., 1996), whereas the forest litter was composed of overlapping layers of impermeable leaves and leaf fragments that almost completely covered the soil surface (forming a smooth surface comparable to a vapour-impermeable plastic sheet with regular perforations to allow rain through) and had its lower layers firmly attached to the surface by fungal hyphae. Although not all forest litter layers are like this (e.g. litter layers where earthworm activity is high, litter in needleleaf forests), litter that provides complete or almost complete ground cover is the norm for moist and wet tropical forests (Molofsky and Augspurger, 1992). Over >1 year, litter enhances soil respiration and therefore may contribute to vapour flow (Sayer et al., 2007), but such longer term effects are not considered here.

In order to match the simulated soil temperature against readings from the control plot (i.e. with litter), it was necessary to increase the rate of thermally-driven soil vapour flow by a factor of m_r =200. Conventionally, heat and vapour flow from a surface are modelled in terms of a single transfer coefficient (aerodynamic resistance) because they are both driven by the movement of turbulent packets of air (eddies, Monteith and Unsworth, 1990) above a thin boundary layer just above the surface where molecular diffusion and then transfer across a laminar flow layer occur (Choudhury and Monteith, 1988). However, this cannot describe an almost continuous and impermeable litter layer that is firmly attached to the surface and will transfer heat but not water. In the SWEAT model, this has resulted in two self-compensating multipliers: one to reduce vapour flow from a litter-covered surface, m_{r1} , and another, m_r , as a correction to allow for the fact that m_{r1} has incorrectly reduced heat flow as well as vapour flow. Gradients in temperature and soil vapour pressure, which drive molecular diffusive flow, are not currently well-described by surface flux models (Marshall et al., 1996; Parlange et al., 1998; Grifoll et al., 2005). The similarity between the behaviour of our forest litter and a perforated plastic sheet is a novel outcome which has not been previously noted: although we had not anticipated this behaviour, we found it to be entirely consistent with our observations of the litter surface.

4.4. Three distinct environments controlled by gap size

The measurements and simulations of this study support a description of three distinct scenarios, controlled by gap size,

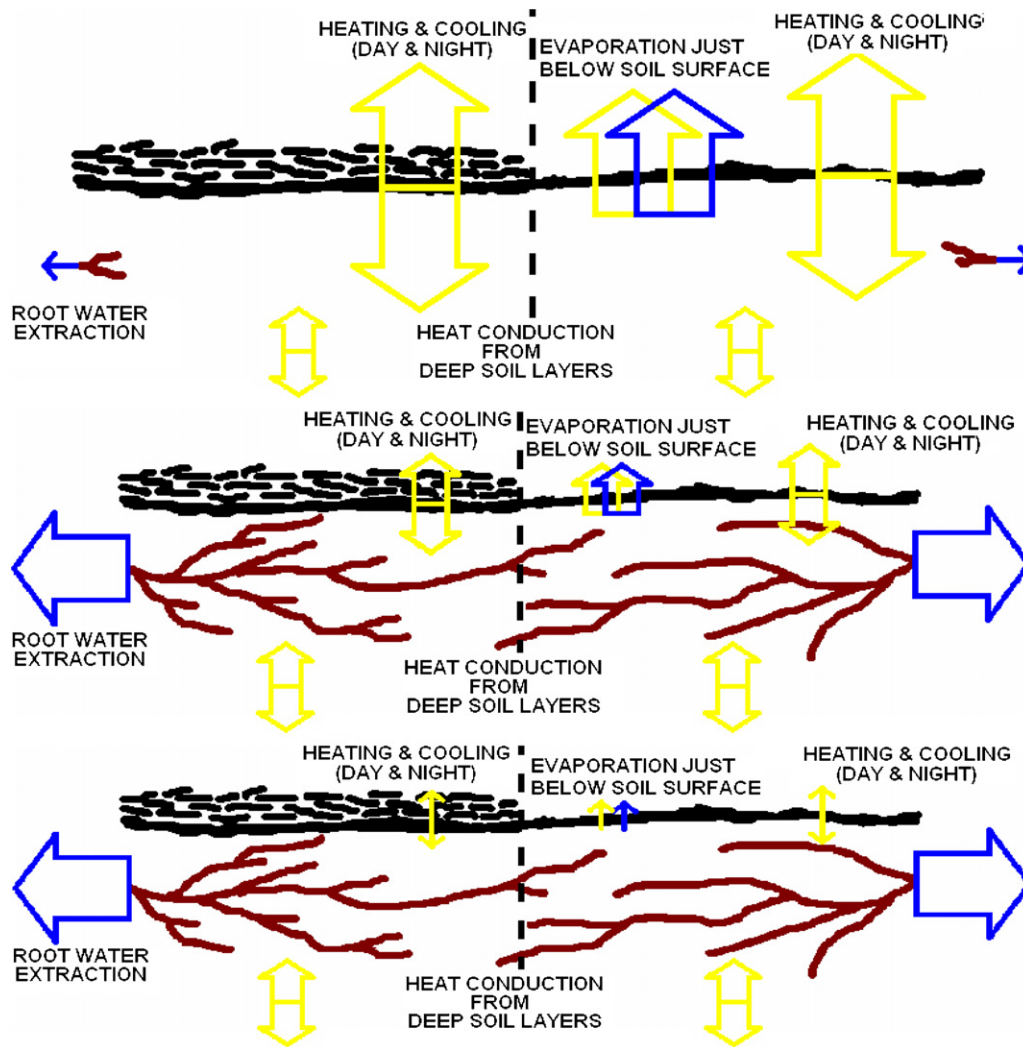


Fig. 9 – Three distinct environments within moist seasonal tropical forests: large gap (red [upper on the black-and-white version of this figure]), small gap (middle) and understorey (blue [lower on the black-and-white version of this figure]), with the above- and below-ground processes that affect soil drying, divided into with-litter (left) and litter-free (right) micro-environments. Movements of water (e.g. root water extraction) are indicated by dark arrows, and movements of heat by light arrows. (For interpretation of the references to color in this figure legend, the reader is referred to the web version of the article.)

of how the above- and below-ground processes that affect soil drying are coupled (Fig. 9):

- In the large gap, root water extraction by surrounding forest trees is negligible so soil drying is dominated by evaporation from the soil surface (blocked in the presence of litter). The soil temperature regime is dominated by direct heating of the soil by sunlight (only slightly affected by litter) and cooling due to evaporation (suppressed by litter).
- In the small gap, root water extraction dominates soil drying (unaffected by litter) with soil evaporation (suppressed by litter) playing a minor role. The soil temperature regime is still dominated by direct sunlight (hardly affected by litter) with some cooling due to evaporation (suppressed by litter).
- In the understorey, root water extraction dominates soil drying (unaffected by litter). The soil temperature regime is dominated by heat conduction from deep soil layers (unaf-

ected by litter) with some evaporation (suppressed by litter) and sensible heat transfer (unaffected by litter).

Although soil type, latitude and season will influence the gap sizes that distinguish between understorey, small and large gap, it seems likely that the same description will apply across most soil types (excluding very swampy soils) in tropical moist forests.

Micro-environments at the soil surface (for bare soil) and within and above the litter layer are the most important during seed germination, but for early seedlings whose roots have penetrated the soil, the scenarios above are of crucial importance. Denslow (1980) categorised tree species as either large gap, small gap or understorey specialists based on seed germination and seedling establishment requirements (cf. Swaine and Whitmore, 1988; Kyereh et al., 1999; Poorter, 2005) and the scenarios presented in this study

might contribute to a mechanistic basis for this division of species.

Additionally, according to these scenarios, the conflicting evidence on whether gaps are drier or wetter than the understorey (Poorter and Hayashida-Oliver, 2000; Poorter, 2005) may be caused by comparisons between environments with contrasting litter cover or between measurements made at different depths (shallow soil at litter-free gap sites should be drier than the understorey because of evaporation, but deeper soil may be wetter if the roots of surrounding trees do not extend very far into the gap). Further research is required to understand fully how much soil dryness controls germination and establishment success in different forest environments (see Hong and Ellis, 1992; Daws et al., 2005a).

4.5. Germination and seedling mortality

Even during the wet season, dry spells of ≥ 6 days occur, on average, 2.5 times a year on BCI and are sufficient to cause increased seedling mortality (Engelbrecht et al., 2006). For seeds that are newly germinated, the challenge is greater than for seedlings because, to survive, the seedling root growth rate must outpace the rate of soil drying. The roots of most seedlings on BCI grow < 50 mm in 5 days and those of most pioneer species < 10 mm in 5 days (Dalling and Hubbell, 2002; Pearson et al., 2003a; Daws et al., 2007), so the dangers of desiccation especially to small (e.g. pioneer) germinating seeds are considerable even in the wet season. For very small seeds (< 1 mg), the risk is compounded by their inability to emerge from beneath litter (Daws et al., 2007). The results of this study show that soil drying would have killed any seedlings attempting to emerge after rainfall during the dry season in a small gap, on bare soil in a large gap, and probably even in small uncovered spaces within the litter layer.

How do seeds avoid this risk? In addition to being dispersed at the end of the dry or start of the wet season, most (but not all) pioneer seeds have germination times > 10 days (median time to germination), implying similarly long times to the critical threshold beyond which a seed is committed to germination (critical imbibition period, Daws et al., 2004). Consequently, at least for the soil type studied, soil drying precludes germination of such seeds during the dry season on BCI, even after heavy rainfall (a notable exception *Ochroma pyramidale* only takes 3.6 days to reach 25% germination, but is only likely to germinate under a highly fluctuating temperature regime, Pearson et al., 2002). The same mechanism may also preclude germination in the early part of the wet season on BCI (when dry spells are most frequent, T-ESP, 2006) and, possibly, also during the *veranillo* ("little summer") period of slightly drier conditions in August–September (Wright and Cornejo, 1990a).

5. Conclusion

From a seed's eye view (Pearson et al., 2003b), three distinct environments are discernible in tropical forests, each with its own balance of above- and below-ground processes affecting soil drying: understorey, small gaps and large gaps. Litter and the roots of surrounding forest trees influence soil water

availability and temperature in all three environments. This framework for understanding tropical forest environments is a development of the standard gap-understorey dichotomy (Whitmore, 1998) and may provide an explanation for apparently conflicting reports on soil water availability in canopy gaps (Poorter and Hayashida-Oliver, 2000; Poorter, 2005), with important consequences for our understanding of seed germination patterns in natural forests. With further research into the mechanisms highlighted here, the welcome result will be a greater understanding of the real significance of gaps in tropical forests, and their role in forest regeneration.

Acknowledgements

This research was supported by the Natural Environment Research Council (studentship to T.R.M. and grant to D.F.R.P.B.), the Center for Tropical Forest Science (grant to C.E.M.) and the Environmental Sciences Program of the Smithsonian Tropical Research Institute (S.T.R.I.) provided funding for F.Y. In the UK, we thank Ilaria Perzia and the staff of the School of Biological Sciences, University of Aberdeen (SBS), especially Martin Wattenbach. In Panama, we thank the STRI staff and fellow researchers on Barro Colorado Island for all their support, especially Jim Dalling and Bob Stallard for the use of their equipment, Raúl Ríos for his valuable assistance in the field, Joe Wright and Egbert Leigh. Thanks to Jérôme Chave and two anonymous reviewers for their comments on earlier drafts of this manuscript.

REFERENCES

- Baillie, I., Elsenbeer, H., Barthold, F., Grimm, R., Stallard, R., 2007. Semi-detailed soil survey of Barro Colorado Island, Panama. http://biogeodb.stri.si.edu/bioinformatics/bci_soil_map.
- Becker, P., Rabenold, P.E., Idol, J.R., Smith, A.P., 1988. Water potential gradients for gaps and slopes in a Panamanian tropical moist forest's dry season. *J. Trop. Ecol.* 4, 173–184.
- Bradford, K.J., 2002. Applications of hydrothermal time to quantifying and modeling seed germination and dormancy. *Weed Sci.* 50, 248–260.
- Brokaw, N.V.L., 1982. The definition of treefall gap and its effect on measures of forest dynamics. *Biotropica* 14, 158–160.
- Brooks, R.H., Corey, A.T., 1964. Hydraulic properties of porous media. Colorado State University Hydrology Papers, vol. 3.
- Bruijnzeel, L.A., 1989. Nutrient cycling in moist tropical forests: the hydrological framework. In: Proctor, J. (Ed.), *Mineral Nutrients in Tropical Forest and Savanna Ecosystems*. Blackwell, Oxford, UK, pp. 383–415.
- Campbell, G.S., 1974. A simple method for determining unsaturated conductivity from moisture retention data. *Soil Sci.* 117, 311–314.
- Campbell, G.S., 1985. *Soil Physics with BASIC*, first ed. Elsevier, Amsterdam, Netherlands.
- Cavelier, J., 1992. Fine-root biomass and soil properties in a semideciduous and a lower montane rain forest in Panama. *Plant Soil* 142, 187–201.
- Chave, J., Condit, R., Lao, S., Caspersen, J.P., Foster, R.B., Hubbell, S.P., 2003. Spatial and temporal variation of biomass in a tropical forest: results from a large census plot in Panama. *J. Ecol.* 91, 240–252.
- Childs, E.C., 1969. *An Introduction to the Physical Basis of Soil Water Phenomena*, first ed. Wiley, London, UK.

- Choudhury, B.J., Monteith, J.L., 1988. A four-layer model for the heat budget of homogeneous land surfaces. *Q. J. R. Meteorol. Soc.* 114, 373–398.
- Condit, R., 1998. *Tropical forest Census Plots: Methods and Results from Barro Colorado Island, Panama and a Comparison with Other Plots*, first ed. Springer, Berlin, Germany.
- Daamen, C.C., 1997. Two source model of surface fluxes for millet fields in Niger. *Agric. For. Meteorol.* 83, 205–230.
- Daamen, C., Simmonds, L., 1994. SWEAT—a numerical model of water and energy fluxes in soil profiles and sparse canopies. Manual. University of Reading, UK.
<http://www.abdn.ac.uk/sweat/DaamenSimmonds1994.pdf>.
- Daamen, C.C., Simmonds, L.P., 1996. Measurement of evaporation from bare soil and its estimation using surface resistance. *Water Resour. Res.* 32, 1393–1402.
- Dalling, J.W., Hubbell, S.P., 2002. Seed size, growth rate and gap microsite conditions as determinants of recruitment success for pioneer species. *J. Ecol.* 90, 557–568.
- Daws, M.I., Ballard, C., Mullins, C.E., Garwood, N.C., Murray, B., Pearson, T.R.H., Burslem, D.F.R.P., 2007. Allometric relationships between seed mass and seedling characteristics reveal trade-offs for neotropical gap-dependent species. *Oecologia* 154, 445–454.
- Daws, M.I., Gaméné, C.S., Glidewell, S.M., Pritchard, H.W., 2004. Seed mass variation potentially masks a single critical water content in recalcitrant seeds. *Seed Sci. Res.* 14, 185–195.
- Daws, M.I., Garwood, N.C., Pritchard, H.W., 2005a. Traits of recalcitrant seeds in a semi-deciduous tropical forest in Panamá: some ecological implications. *Funct. Ecol.* 19, 874–885.
- Daws, M.I., Mullins, C.E., Burslem, D.F.R.P., Paton, S.R., Dalling, J.W., 2002. Topographic position affects the water regime in a semideciduous tropical forest in Panamá. *Plant Soil* 238, 79–90.
- Daws, M.I., Pearson, T.R.H., Burslem, D.F.R.P., Mullins, C.E., Dalling, J.W., 2005b. Effects of topographic position, leaf litter and seed size on seedling demography in a semi-deciduous tropical forest in Panamá. *Plant Ecol.* 179, 93–105.
- Deka, R.N., Wairiu, M., Mtakwa, P.W., Mullins, C.E., Veenendaal, E.M., Townend, J., 1995. Use and accuracy of the filter-paper technique for measurement of soil matric potential. *Eur. J. Soil Sci.* 46, 233–238.
- Denslow, J.S., 1980. Gap partitioning among tropical rainforest trees. *Biotropica* 12 (Suppl.), 47–55.
- Dietrich, W.E., Windsor, D.M., Dunne, T., 1982. Geology, climate, and hydrology of Barro Colorado Island. In: Leigh, E.G., Rand, A.S., Windsor, D.M. (Eds.), *The Ecology of a Tropical Forest Seasonal Rhythms and Long-term Changes*. Smithsonian, Washington, DC, pp. 21–46.
- Dirksen, C., 2001. Unsaturated hydraulic conductivity. In: Smith, K.A., Mullins, C.E. (Eds.), *Soil and Environmental Analysis: Physical Methods*, second ed. Marcel Dekker, New York, pp. 183–237.
- Engelbrecht, B.M.J., Dalling, J.W., Pearson, T.R.H., Wolf, R.L., Gálvez, D.A., Koehler, T., Ruiz, M.C., Kursar, T.A., 2001. Short dry spells in the wet season increase mortality of tropical pioneer seedlings. In: Ganeshaiah, K.N., Shaanker, R.U., Bawa, K.S. (Eds.), *Tropical Ecosystems: Structure, Diversity and Human Welfare*. Oxford & IBH Publishing, New Delhi, India, pp. 665–669.
- Engelbrecht, B.M.J., Dalling, J.W., Pearson, T.R.H., Wolf, R.L., Gálvez, D.A., Koehler, T., Tyree, M.T., Kursar, T.A., 2006. Short dry spells in the wet season increase mortality of tropical pioneer seedlings. *Oecologia* 148, 258–269.
- Foster, R.B., Brokaw, N.V.L., 1982. Structure and history of the vegetation of Barro Colorado Island. In: Leigh, E.G., Rand, A.S., Windsor, D.M. (Eds.), *The Ecology of a Tropical Forest Seasonal Rhythms and Long-term Changes*. Smithsonian, Washington, DC, pp. 67–81.
- Garwood, N.C., 1983. Seed germination in a seasonal tropical forest in Panama: a community study. *Ecol. Monogr.* 53, 159–181.
- Grifoll, J., Gastó, J.M., Cohen, Y., 2005. Non-isothermal soil water transport and evaporation. *Adv. Water Resour.* 28, 1254–1266.
- Grubb, P.J., 1996. Rainforest dynamics: the need for new paradigms. In: Edwards, D.S., Booth, W.E., Choy, S.C. (Eds.), *Tropical Rainforest Research—Current Issues*. Kluwer, Dordrecht, Netherlands, pp. 215–233.
- Gummerson, R.J., 1986. The effect of constant temperatures and osmotic potentials on the germination of sugar beet. *J. Exp. Bot.* 37, 729–741.
- Holdridge, L.R., Grenke, W.C., Hatheway, W.H., Liang, T., Tosi, J.A., 1971. *Forest Environments in Tropical Life Zones*, first ed. Pergamon Press, Oxford, UK.
- Hong, T.D., Ellis, R.H., 1992. The survival of germinating orthodox seeds after desiccation and hermetic storage. *J. Exp. Bot.* 43, 239–247.
- Hubbell, S.P., Foster, R.B., 1983. Diversity of canopy trees in a neotropical forest and implications for conservation. In: Sutton, S.L., Whitmore, T.C., Chadwick, A.C. (Eds.), *Tropical Rain Forest: Ecology and Management*. Blackwell, Oxford, UK, pp. 25–41.
- Hubbell, S.P., Foster, R.B., O'Brien, S.T., Harms, K.E., Condit, R., Wechsler, B., Wright, S.J., de Lao, S.L., 1999. Light-gap disturbances, recruitment limitation, and tree diversity in a neotropical forest. *Science* 283, 554–557.
- Johnsson, M.J., Stallard, R.F., 1989. Physiographic controls on the composition of sediments derived from volcanic and sedimentary terrains on Barro Colorado Island Panama. *J. Sediment. Petrol.* 59, 768–781.
- Jordan, C.F., 1993. Ecology of tropical forests. In: Pancel, L. (Ed.), *Tropical Forestry Handbook*, vol. 1. Springer, Berlin, Germany, pp. 165–197.
- Kyereh, B., Swaine, M.D., Thompson, J., 1999. Effect of light on the germination of forest trees in Ghana. *J. Ecol.* 87, 772–783.
- Leigh, E.G., 1999. Tropical climates. In: Leigh, E.G. (Ed.), *Tropical Forest Ecology: A View from Barro Colorado Island*. OUP, New York, pp. 46–66.
- Marshall, T.J., Holmes, J.W., Rose, C.W., 1996. *Soil Physics*, third ed. CUP, Cambridge, UK.
- Molofsky, J., Augspurger, C.K., 1992. The effect of leaf litter on early seedling establishment in a tropical forest. *Ecology* 73, 68–77.
- Monteith, J.L., Unsworth, M.H., 1990. *Principles of Environmental Physics*, second ed. Butterworth, Oxford, UK.
- Mullins, C.E., 2001. Matric potential. In: Smith, K.A., Mullins, C.E. (Eds.), *Soil and Environmental Analysis: Physical Methods*, second ed. Marcel Dekker, New York, pp. 65–93.
- Mullins, C.E., Townend, J., Mtakwa, P.W., Payne, C.A., Cowan, G., Simmonds, L.P., Daamen, C.C., Dunbabin, T., Naylor, R.E.L., 1996. EMERGE—a model to predict crop emergence in the semi-arid tropics. *Users' Guide*. University of Aberdeen, UK.
- Ostertag, R., 1998. Belowground effects of canopy gaps in a tropical wet forest. *Ecology* 79, 1294–1304.
- Parlange, M.B., Cahill, A.T., Nielsen, D.R., Hopmans, J.W., Wendroth, O., 1998. Review of heat and water movement in field soils. *Soil Till. Res.* 47, 5–10.
- Pearson, T.R.H., Burslem, D.F.R.P., Goeriz, R.E., Dalling, J.W., 2003a. Interactions of gap size and herbivory on establishment, growth and survival of three species of neotropical pioneer trees. *J. Ecol.* 91, 785–796.
- Pearson, T.R.H., Burslem, D.F.R.P., Mullins, C.E., Dalling, J.W., 2002. Germination ecology of neotropical pioneers: interacting

- effects of environmental conditions and seed size. *Ecology* 83, 2798–2807.
- Pearson, T.R.H., Burslem, D.F.R.P., Mullins, C.E., Dalling, J.W., 2003b. Functional significance of photoblastic germination in neotropical pioneer trees: a seed's eye view. *Funct. Ecol.* 17, 394–402.
- Poorter, L., 2005. Resource capture and use by tropical forest tree seedlings and their consequences for competition. In: Burslem, D.F.R.P., Pinard, M.A., Hartley, S.E. (Eds.), *Biotic Interactions in the Tropics: Their Role in the Maintenance of Species Diversity*. CUP, Cambridge, UK, pp. 35–64.
- Poorter, L., Hayashida-Oliver, Y., 2000. Effects of seasonal drought on gap and understorey seedlings in a Bolivian moist forest. *J. Trop. Ecol.* 16, 481–498.
- R Development Core Team, 2006. R: a language and environment for statistical computing, version 2.3.1. R Foundation for Statistical Computing, Vienna. URL <http://www.R-project.org>.
- Rand, A.S., Rand, W.M., 1982. Variation in rainfall on Barro Colorado Island. In: Leigh, E.G., Rand, A.S., Windsor, D.M. (Eds.), *The Ecology of a Tropical Forest Seasonal Rhythms and Long-term Changes*. Smithsonian, Washington, DC, pp. 47–59.
- Sayer, E.J., 2005. Using experimental manipulation to assess the roles of leaf litter in the functioning of forest ecosystems. *Biol. Rev.* 80, 1–31.
- Sayer, E.J., Tanner, E.V.J., Cheeseman, A.W., 2006. Increased litterfall changes fine root distribution in a moist tropical forest. *Plant Soil* 281, 5–13.
- Sayer, E.J., Powers, J.S., Tanner, E.V.J., 2007. Increased litterfall in tropical forests boosts the transfer of soil CO₂ to the atmosphere. *PloS ONE* 12, e1299.
- Shao, Y., Irannejad, P., 1999. On the choice of soil hydraulic models in land-surface schemes. *Boundary Layer Meteorol.* 90, 83–115.
- Swaine, M.D., Whitmore, T.C., 1988. On the definition of ecological species groups in tropical rain forests. *Vegetatio* 75, 81–86.
- T-ESP, 2006. Terrestrial-Environmental Sciences Program. Smithsonian Tropical Research Institute, Panama. URL http://striweb.si.edu/esp/physical_monitoring/download_bci.htm.
- Townend, J., Reeve, M.J., Carter, A., 2001. Water release characteristic. In: Smith, K.A., Mullins, C.E. (Eds.), *Soil and Environmental Analysis: Physical Methods*, second ed. Marcel Dekker, New York, pp. 95–140.
- van der Meer, P.J., Bongers, F., 1996. Patterns of tree-fall and branch-fall in a tropical rain forest in French Guiana. *J. Ecol.* 84, 19–29.
- van der Meer, P.J., Bongers, F., Chatrou, L., Riéra, B., 1994. Defining canopy gaps in a tropical rain forest: effects on gap size and turnover time. *Acta Oecol.* 15, 701–714.
- van Genuchten, M.T., 1980. A closed-form equation for predicting the hydraulic conductivity of unsaturated soils. *Soil Sci. Soc. Am. J.* 44, 892–898.
- Veenendaal, E.M., Swaine, M.D., Agyeman, V.K., Blay, D., Abebrese, I.K., Mullins, C.E., 1996. Differences in plant and soil water relations in and around a forest gap in West Africa during the dry season may influence seedling establishment and survival. *J. Ecol.* 84, 83–90.
- Welden, C.W., Hewett, S.W., Hubbell, S.P., Foster, R.B., 1991. Sapling survival, growth, and recruitment: relationship to canopy height in a neotropical forest. *Ecology* 72, 35–50.
- Whitmore, T.C., 1998. *An Introduction to Tropical Rain Forests*, second ed. OUP, New York.
- Wright, S.J., Cornejo, F.H., 1990a. Seasonal drought and leaf fall in a tropical forest. *Ecology* 71, 1165–1175.
- Wright, S.J., Cornejo, F.H., 1990b. Seasonal drought and the timing of flowering and leaf fall in a neotropical forest. In: Bawa, K.S., Hadley, M. (Eds.), *Reproductive Ecology of Tropical Forest Plants*. UNESCO & Parthenon, Paris, France, pp. 49–61.
- Yavitt, J.B., 2000. Nutrient dynamics of soil derived from different parent material on Barro Colorado Island, Panama. *Biotropica* 32, 198–207.